Performance Characteristics for an Array of Two Receiving Systems With Unequal Predetection Signal-to-Noise Ratios and Enhanced Radio Frequency Carrier Margin Improvement

M. H. Brockman
Telecommunications Science and Engineering Division

Enhanced radio frequency carrier margin improvement for arrayed receiving systems for coherent reception of phase modulated signals with residual carrier provides a significant reduction in carrier loop phase noise and increase in signal-to-noise ratio in the RF carrier tracking loop with an attendant reduction in telemetry radio loss. A significant increase in doppler frequency rate capability is also realized relative to operating at a narrower tracking loop bandwidth to obtain the same carrier sensitivity improvement. This report examines these performance characteristics for an array of two receiving systems with unequal apertures and statistically independent predetection noise.

I. Introduction

An earlier report (Ref. 1) presented a technique for providing enhanced radio frequency carrier margin improvement for coherent carrier reception and demodulation of phase modulated signals with residual carrier for an array of receiving systems with unequal antenna apertures. This report presents additional performance information for receiver design parameters and with array parameters representative of a 34-meter-diameter high-efficiency (listen only) antenna receiving system arrayed with a 64-meter-diameter antenna-receiving system. In this report, the various components of operating system noise temperature (T_{op}) are treated as statistically independent among the receiving systems of the array (as in Ref. 1).

The information presented in this report provides additional performance characteristics for the RF carrier phase tracking loop to illustrate the manner in which the enhanced RF carrier margin improvement performance characteristics for an array shown in Ref. 1 were obtained for a given set of design parameters Performance characteristics are presented herein that show RF carrier tracking loop phase noise reduction and signal-to-noise ratio improvement (e.g., 3.2 db) as well as enhanced RF carrier margin improvement (e.g., 4.8 db). In addition, performance characteristics are shown to illustrate the increase in doppler rate capability realized (i e , 2.9 times) relative to that obtained by switching to a narrower tracking loop bandwidth to obtain the same RF carrier signal level sensitivity improvement

The performance characteristics presented in this report apply to a second order RF carrier phase tracking loop which includes a bandpass limiter and a sinusoidal phase detector. The technique presented herein is also applicable to higher order tracking loops and to digitally implemented tracking loops that incorporate a bandpass limiter or equivalent at an intermediate frequency (IF) in each of the receiving systems of the array.

II. Receiver Configuration

Figure 1 illustrates a method for achieving RF carrier arraying (Ref. 1, Fig. 1). A modification of Fig. 1 (so that much larger antenna separation for the array can be handled conveniently) was presented in Ref. 2 with a discussion of predetection noise resulting from operating equivalent system noise temperature T_{op}. Figure 2 illustrates a second configuration that provides additional filtering of receiving system 2 (through N) local oscillator phase noise which couples into receiving system 1 via the RF carrier summing junction. Consequently, Fig. 2 generally provides an increase in carrier margin relative to Fig 1. The received signal is an RF carrier (ω_{RF}) phase modulated with a square-wave subcarrier (ω_{sc}) at a peak modulation index m_{pd} that is, in turn, biphase modulated with data $D(t)$.

$$\underbrace{2^{1/2} A \cos m_{pd} \cos \omega_{RF} t}_{\text{carrier}} + \underbrace{2^{1/2} A \sin m_{pd} \times D(t) \times \left[\cos (\omega_{sc} t) \times \sin \omega_{RF} t + n(t)\right]}_{\text{sidebands}} \quad (1)$$

The term $n(t)$ represents receiver noise which has a double-sided noise spectral density $N_o/2$.

III. Predetection Signal-to-Noise Ratio and RF Carrier Tracking Loop Phase Noise

The improvement in predetection carrier power-to-noise spectral density in receiving system 1 for two receiving systems arrayed (η_2) is

$$\eta_2 = \frac{\left[1 + \beta_2 \gamma_2 \left(\frac{N_{o2}}{N_{o1}}\right)^{1/2}\right]^2}{\left[1 + \frac{N_{o2}}{N_{o1}} \beta_2^2\right]} \quad (2)$$

where β_2 is the voltage coupling of receiving system 2 relative to receiving system 1 at the summing junction. The term γ_2^2 is the ratio of the carrier power-to-noise spectral density ratio of receiving system 2 relative to the carrier power-to-noise spectral density ratio of receiving system 1. Receiving system 1 has a double-sided noise spectral density $N_{o1}/2$ related to T_{op1} and receiving system 2 has a double-sided noise spectral density $N_{o2}/2$ related to T_{op2}. Note that for N receiving systems

$$\eta_N = \frac{\left[1 + \beta_2 \gamma_2 \left(\frac{N_{o2}}{N_{o1}}\right)^{1/2} + \cdots + \beta_N \gamma_N \left(\frac{N_{oN}}{N_{o1}}\right)^{1/2}\right]^2}{\left[1 + \frac{N_{o2}}{N_{o1}} \beta_2^2 + \cdots + \frac{N_{oN}}{N_{o1}} \beta_N^2\right]} \quad (3)$$

It should be noted that in Ref. 1, the terms $(N_{o2}/N_{o1})^{1/2}$ and $(N_{oN}/N_{o1})^{1/2}$ in the numerators of expressions (2) and (3) above should have been included in expressions (1), (2), (7), (8), (11) and (12) This omission was also made in expressions (2), (3), (4) and (5) of Ref. 3. For the system noise temperature ratios in Refs. 1 and 3 and the antenna spacings and orientation planned for the 64- and 34-m antennas at the three DSN complexes, the omission described above represents a 0.1 db error in the results presented.

Consider the RF carrier phase tracking loop in receiving system 1 for the situation where the predetection IF filters F_{A2} through F_{AN} in receiving systems 2 through N have k times the noise bandwidth of predetection filter F_{A1} in receiving system 1 (see Ref. 1) The RF carrier tracking loop is a second-order phase tracking loop which includes a bandpass limiter and a sinusoidal phase detector. With receiving system 1 only connected to the summing junction, the resultant rms phase noise ($\sigma_{\phi_{n1}}$) at the output of the RF carrier tracking loop (i.e., on the first local oscillator) becomes (Ref. 1, Expression [4b]):

$$\sigma_{\phi_{n1}} = \frac{\frac{N_{o1}}{2} \cdot 2B_{L_1}}{P_{c_1}} \times \left[\frac{1 + \frac{P_{c_1}}{NBW_{F_{A1}} \cdot N_{o1}}}{0.862 + \frac{P_{c_1}}{NBW_{F_{A1}} \cdot N_{o1}}} \cdot \frac{\exp\left(\frac{N_{o1} B_{L_1}}{P_{c_1}}\right)}{\sinh\left(\frac{N_{o1} B_{L_1}}{P_{c_1}}\right)}\right]^{1/2}$$

radians, rms (4)

where $P_{c1}/NBW_{F_{A1}} \cdot N_{o1}$) is the RF carrier signal-to-noise power ratio at the input to the bandpass limiter in the carrier phase tracking loop. The term $NBW_{F_{A1}}$ represents the noise bandwidth of predetection IF filter F_{A1} in receiving system 1. The two-sided closed-loop noise bandwidth can be expressed as:

$$2B_{L1} = \frac{2B_{Lo1}}{r_o + 1}\left(1 + r_o \frac{\alpha_1}{\alpha_{o1}}\right) \tag{5}$$

where $r_o = 2$ by design at design point (0.707 damping) and $2B_{L_{o1}}$ is the design point (threshold) two-sided closed-loop noise bandwidth in receiving system 1. The term α_1 is the limiter suppression factor resulting from the noise-to-carrier power ratio due to $NBW_{F_{A1}}$ at the input to the bandpass limiter. The suppression factor α_1 has a value of α_{o1} at design point (threshold). At threshold, the predetection carrier-to-noise power ratio in a noise bandwidth equal to $2B_{L_{o1}}$ is unity (i.e., $P_c/(2B_{L_o} \cdot N_o) = 1$).

With receiving systems 1 and 2 connected to the summing junction, the RF carrier signal-to-noise power ratio at the input to the bandpass limiter is (Ref. 1, Expression 6)

$$\frac{P_{c1_{\Sigma 1,2}}}{P_{n1_{\Sigma 1,2}}} = \frac{(A_1 \cos m_{pd} + \beta_2 A_2 \cos m_{pd})^2}{\left[NBW_{F_{A1}} \cdot N_{o1} + \beta_2^2 NBW_{F_{A2}} \cdot N_{o2}\right]} \tag{6}$$

where m_{pd} is the peak phase modulation index, and $NBW_{F_{A2}} = k_2 \cdot NBW_{F_{A1}}$. Expression (6) can be rewritten as:

$$\frac{P_{c1_{\Sigma 1,2}}}{P_{n1_{\Sigma 1,2}}} = \frac{P_{c1}}{NBW_{F_{A1}} \cdot N_{o1}} \cdot \frac{\left[1 + \beta_2 \gamma_2 \left(\frac{N_{o2}}{N_{o1}}\right)^{1/2}\right]^2}{\left[1 + \frac{N_{o2}}{N_{o1}} \beta_2^2 k_2\right]} \tag{7}$$

The change in RF carrier signal-to-noise power ratio at the input to the bandpass limiter in receiving system 1 is then:

$$\Delta_2 = \frac{\left[1 + \beta_2 \gamma_2 \left(\frac{N_{o2}}{N_{o1}}\right)^{1/2}\right]^2}{\left[1 + \frac{N_{o2}}{N_{o1}} \beta_2^2 k_2\right]} \tag{8}$$

The limiter suppression factor due to the change in noise-to-carrier power ratio becomes $\alpha_{1_{\Delta 2}}$ which provides a two-sided closed-loop noise bandwidth.

$$2B_{L1_{\Delta 2}} = \frac{2B_{L_{o1}}}{r_o + 1}\left(1 + r_o \frac{\alpha_{1_{\Delta 2}}}{\alpha_{o1}}\right) \tag{9}$$

The resultant rms phase noise at the output of the RF carrier tracking loop (i e., on the first local oscillator) in receiving system 1 becomes.

$$\sigma_{\phi_{n1\Sigma 1,2}} = \frac{\frac{N_{o1}}{2} \cdot 2B_{L1_{\Delta 2}}}{P_{c1}} \cdot \frac{1}{\eta_2} \cdot \left[\frac{1 + \frac{P_{c1} \cdot \Delta_2}{NBW_{F_{A1}} \cdot N_{o1}}}{0\,862 + \frac{P_{c1} \cdot \Delta_2}{NBW_{F_{A1}} \cdot N_{o1}}} \cdot \frac{\exp\left(\frac{N_{o1} \cdot B_{L1_{\Delta 2}}}{P_{c1} \cdot \eta_2}\right)}{\sinh\left(\frac{N_{o1} \cdot B_{L1_{\Delta 2}}}{P_{c1} \cdot \eta_2}\right)}\right]^{1/2} \text{ rad, rms} \tag{10}$$

Note that the total rms phase noise at the output of the RF carrier tracking loop (i.e , on the first local oscillator) in receiving system 1 for Fig. 1 (Ref. 1) is:

$$\left[\sigma^2_{\phi_{n1\Sigma 1,2}} + \left(\frac{\beta_2 \sigma_{\phi_{n2}}}{1 + \beta_2}\right)^2\right]^{1/2} \tag{11}$$

In Fig. 2, additional filtering of the output rms phase noise $\sigma_{\phi_{n2}}$ is provided by the local oscillator tracking loop in receiving system 2. Designate the additionally filtered rms phase noise as $\sigma'_{\phi_{n2}}$ which is less than $\sigma_{\phi_{n2}}$ by the square root of the ratio of local oscillator tracking loop noise bandwidth to $2B_{L2}$. Consequently for Fig. 2, $\sigma'_{\phi_{n2}}$ is substituted into expression (11) in place of $\sigma_{\phi_{n2}}$. Note that since receiving system 2 has the same first local oscillator as receiving system 1, receiving system 2 has effectively the same RF carrier characteristics and sensitivity as receiving system 1.

The rms phase noise (Expression [11]) represents a different RF carrier margin when compared to $\sigma_{\phi_{n1}}$ for receiving system 1 alone (Expression [4]). The change in RF carrier margin represents the enhanced carrier margin improvement for two receiving systems arrayed.

The RF carrier phase tracking loop in receiving system 2 is also a second-order phase tracking loop ($r_o = 2$) which utilized a bandpass limiter and sinusoidal phase detector. Since the closed loop noise bandwidth of the carrier phase tracking loop for receiving systems 2 through N is much narrower (by design) than that in receiving system 1, phase noise in receiving system 1 carrier tracking loop produces a reduction in predetection carrier signal-to-noise ratio in receiving systems 2 through N. The resultant predetection carrier signal-to-noise ratio in receiving system 2 for two systems arrayed is then

$$\frac{P_{c2\Sigma 1,2}}{P_{n_2}} = \frac{P_{c_2}\left(1 - \frac{\sigma^2_{\phi_{n1\Sigma 1,2}}}{2}\right)^2}{NBW_{F_{A2}} \cdot N_{o2}} \tag{12}$$

which produces an rms phase noise

$$\sigma_{\phi_{n2\Sigma 1,2}} = \frac{\frac{N_{o2}}{2} \cdot 2B_{L2}}{P_{c_{2\Sigma 1,2}}} \times \left[\frac{1 + \frac{P_{c2\Sigma 1,2}}{NBW_{F_{A2}} \cdot N_{o2}}}{0.862 + \frac{P_{c2\Sigma 1,2}}{NBW_{F_{A2}} \cdot N_{o2}}} \cdot \frac{\exp\left(\frac{N_{o2} \cdot B_{L2}}{P_{c2\Sigma 1,2}}\right)}{\sinh\left(\frac{N_{o2} \cdot B_{L2}}{P_{c2\Sigma 1,2}}\right)}\right]^{1/2} \text{ rad, rms} \tag{13}$$

IV. Performance

Performance characteristics are presented in this report for an array of two receiving systems with a 64-meter-diameter antenna (system 1) and a 34-meter-diameter high-efficiency (listen only) antenna (system 2) with $\gamma_2 = 0.61$ (-4.3 db), $k_2 = 9$, $N_{o2}/N_{o1} = 0.925$ and $\beta_2 = 1.0$. Design parameters for receiving system 1 are $2B_{Lo1} = 30$ Hz and $NBW_{FA1} = 2000$ Hz while design parameters for receiving system 2 are $2B_{Lo2} = 1.0$ Hz and $NBW_{FA2} = k_2 \cdot NBW_{FA1}$. The local oscillator tracking loop for receiving system 2 (Fig. 2) has a two-sided noise bandwidth of 1.0 Hz.

Figure 3 shows the rms phase noise $\sigma_{\phi_{n1}}$ at the output of the RF carrier tracking loop (i.e., on the first local oscillator) for receiving system 1 by itself. Phase noise is shown as a function of initial 64-m receiver RF carrier margin (carrier level above design point) as calculated from Expression (4) above using the design parameters in the preceding paragraph. Figure 3 also shows the total rms phase noise (Expression [11]) at the output of the RF carrier tracking loop in receiving system 1 for an array of two receiving systems with a 64-meter-diameter antenna (system 1) and a 34-meter-diameter high-efficiency (listen-only) antenna (system 2). Total rms phase noise is shown for array configurations that are representative of Figs. 1 and 2 with $k_2 = 9$.

Note, in Fig. 3, that with receiving system 1 by itself (prior to arraying) initially at 5.5 db above design point threshold (carrier margin), the rms phase noise for the array is 21.9 and 21.7 degrees respectively for array configurations representative of Figs. 1 and 2 ($k_2 = 9$). These rms phase noise levels (21.9 and 21.7 degrees) when compared to the phase noise characteristic of system 1 by itself represent an enhanced RF carrier margin of 10.1 and 10.3 db, respectively. The improvement in the 64-m receiver (system 1) carrier margin is then 4.6 and 4.8 db, respectively, with receiving system 1 and 2 arrayed (see Fig. 7, Ref. 1, $k = 9$). Note that the difference in carrier margin improvement for Fig. 2 relative to Fig. 1 increases for three receiving systems arrayed (see Fig 15, Ref. 1). Figure 4 shows receiver array enhanced RF carrier margin versus initial 64-m receiver RF carrier margin for the array described above.

Consider the RF carrier tracking loop signal-to-noise ratio (SNR) for receiving system 1 by itself. Using the linear theoretical model (Refs. 4 and 5):

$$\rho_{L1} = \frac{P_{c1}}{N_{o1} B_{L1} \Gamma_1} \tag{14}$$

where ρ_{L1} is the RF carrier loop SNR for receiving system 1 (64 m) by itself and Γ_1 is the bandpass limiter performance factor:

$$\Gamma_1 = \frac{1 + \frac{P_{c1}}{NBW_{F_{A1}} N_{o1}}}{0.862 + \frac{P_{c1}}{NBW_{F_{A1}} N_{o1}}} \tag{15}$$

Figure 5 shows the RF carrier loop SNR for receiving system 1 by itself (ρ_{L1}) as a function of initial 64-m receiver RF carrier margin as calculated from Expression (14). Note the interrelationship provided by Figs. 3 and 5 between rms phase noise at the output of the RF carrier tracking loop and tracking loop SNR. Using this relationship, the total rms phase noise (Expression [11]) at the output of the RF carrier tracking loop in receiving system 1 for the two receiver array provides the RF carrier loop SNR in receiving system 1 also

shown in Fig. 5 for array configurations representative of Figs. 1 and 2 with $k_2 = 9$ and design parameters as discussed above. Using the linear theoretical model for the array.

$$\rho_{L1\Sigma 1,2} = \frac{P_{c1}\,\eta_2}{N_{o1}\,B_{L1_{\Delta 2}}\,\Gamma_{1_{\Delta 2}}} \tag{16}$$

where

$$\Gamma_{1_{\Delta 2}} = \frac{1 + \dfrac{P_{c1}\cdot\Delta_2}{NBW_{F_{A1}}\cdot N_{o1}}}{0.862 + \dfrac{P_{c1}\cdot\Delta_2}{NBW_{F_{A1}}\cdot N_{o1}}} \tag{17}$$

The RF carrier loop SNR for receiving system 1 for the two receiver array calculated from Expression (16) provides essentially the same curve as the array configuration representative of Fig. 2 shown in Fig 5. This results from the additional local oscillator filtering in receiving system 2. Note the 3.2 db improvement in the 64-m receiving system (system 1) RF carrier tracking loop signal-to-noise ratio in Fig. 5 for the two-receiver array relative to system 1 by itself initially at 10 db above design point threshold (carrier margin). Reduction in RF carrier loop rms phase noise (Fig. 3) and resultant improvement in carrier loop SNR (Fig. 5) provide an attendant reduction in telemetry radio loss (Refs. 1, and 5).

The reduction in rms phase noise on the first local oscillator (system 1) for the receiver array shown in Fig. 3 (with $2B_{Lo1} = 30$ Hz) raises the point of switching to a narrower bandwidth in the RF carrier tracking loop to accomplish essentially the same reduction in rms phase noise. Switching system 1 (64 m) by itself to a $2B_{Lo1}$ of 10 Hz improves its carrier margin by 30/10 or 4.77 db relative to operation with $2B_{Lo1} = 30$ Hz. This narrower closed-loop noise bandwidth provides very nearly the same rms phase noise as the array in Fig. 3. Consider the following discussion.

Figure 6 shows the two-sided closed-loop noise bandwidth $2B_{L1}$ (Expression [5]) of the RF carrier tracking loop for receiving system 1 (64 m) by itself as a function of initial 64-m receiver carrier margin for $2B_{Lo1} = 30$ Hz. Figure 6 also shows the two-sided closed-loop noise bandwidth $2B_{L1\Delta 2}$ (Expression [9]) for the array of two receiving systems described above with $k_2 = 9$. Note the 5.5 db offset in RF carrier level of $2B_{L1\Delta 2}$ relative to $2B_{L1}$. Doppler rate capability (for a 10 degree phase error due to doppler rate) is shown in Fig. 7 for receiving system 1 by itself as a function of initial 64-m receiver carrier margin for $2B_{Lo1} = 30$ Hz. Figure 7 also shows the resulting doppler rate capability for the array described above for a 10 degree phase error ($k_2 = 9$). Note the 5.5 db offset in RF carrier level between the doppler rate curves. Finally, Fig. 8 shows the doppler rate capability for a 10 degree phase error as a function of RF carrier margin for $2B_{Lo1} = 10$ Hz. The information for two-sided noise bandwidth and doppler rate capability is contained in JPL Document 810-5, Rev. D, *Deep Space Network/Flight Project Interface Design Handbook*, Volume 1, TRK 20, (internal document).

Consider an initial RF carrier margin of 10 db for receiving system 1 (64 m) by itself with $2B_{Lo1} = 30$ Hz. The doppler rate capability for an array of two receiving systems ($k_2 = 9.0$) is 37.5 Hz/s for a 10 degree phase error (Fig. 7). In Fig. 8, the corresponding RF carrier margin for $2B_{Lo1} = 10$ Hz is 14.77 db. At this carrier margin, the doppler rate capability for a 10 degree phase error is 12.8 Hz/s. Consequently the array of two receiving systems with $2B_{Lo1} = 30$ Hz and $k_2 = 9$ has a doppler rate capability of 37.5/12.8 or 2.9 times the doppler rate capability of receiving system 1 by itself operating with a $2B_{Lo1}$ of 10 Hz. With an array of two receiving systems for $2B_{Lo1} = 10$ Hz with $k_2 = 1$, the above ratio becomes 2.6.

Performance characteristics for the RF carrier tracking loop in receiving system 2 (34 m) are shown in Figs. 9 and 10 for the design parameters shown above. Figure 9 shows the rms phase noise $\sigma_{\phi n2}$ at the output of the RF carrier tracking loop for receiving system 2 by itself. Phase noise is shown as a function of initial 34-m receiver carrier margin (carrier level above design point for $k_2 = 1.0$) as calculated from Expression (13) above. Figure 9 also shows rms phase noise for $k_2 = 9$, as calculated from Expression (13). The corresponding two-sided closed-loop noise bandwidth $2B_{L2}$ is shown in Fig. 10 for $k_2 = 1.0$ and 9.0 as a function of initial 34-m receiver carrier margin (carrier level above design point for $k_2 = 1.0$). Taking into account the effect of Expression (12) and γ_2, the information shown in Figs. 9 and 10 for $k_2 = 9$ permits calculation of total rms phase noise (Expression [11]) at the output of the RF carrier tracking loop in receiving system 1 for array configurations representative for Figs. 1 and 2.

V. Discussion

Enhanced RF carrier margin improvement for an array representative of a 34-meter-diameter high-efficiency (listen only) antenna receiving system and a 64-meter-diameter antenna receiving system with $k_2 = 9$ is presented in this report. With an initial RF carrier margin of 10 db for the 64-m receiving system (by itself) with $2B_{Lo1} = 30$ Hz, the enhanced RF carrier margin improvement is 4.8 db and 5 0 db (Figs. 1 and 2 configurations, respectively). This enhanced carrier margin im-

provement (4.8 and 5.0 db) is realized with an improvement in predetection signal power-to-noise spectral density in receiving system 1 of 1.2 db. The corresponding improvement in RF carrier tracking loop signal-to-noise ratio improvement is 3.15 db and 3.25 db (Fig. 5). In addition, the array has 2.9 times the doppler rate capability relative to operating the 64-m receiving system with $2B_{L_{o1}} = 10$ Hz.

The additional RF carrier sensitivity realized by enhanced carrier margin improvement provides a performance capability that should be investigated and verified by further Laboratory investigation including operation at initial carrier margins (prior to arraying) of less than 10 db. In light of the performance shown in this report, the array presented herein should acquire the RF carrier when the initial 64-m receiver carrier margin is as low as 5.5 db. After RF acquisition at this signal level, the effective RF carrier margin of the array would be 10.2 db (Fig. 4) as determined by rms phase noise at the output of the RF carrier phase tracking loop (i.e., on the first local oscillator).

References

1. Brockman, M. H., "Enhanced Radio Frequency Carrier Margin Improvement for an Array of Receiving Systems with Unequal Predetection Signal-to-Noise Ratios," *TDA Progress Report 42-76*, pp. 170-188, Jet Propulsion Laboratory, Pasadena, California, February 15, 1984.

2 Brockman, M. H., "The Effect of Partial Coherence in Receiving System Noise Temperature on Array Gain for Telemetry and Radio Frequency Carrier Reception for Similar Receiving Systems," *TDA Progress Report 42-66*, pp. 219-235, Jet Propulsion Laboratory, Pasadena, California, December 15, 1981.

3. Brockman, M. H., "The Effect of Partial Coherence in Receiving System Noise Temperature on Array Gain for Telemetry and Radio Frequency Carrier Reception for Receiving Systems with Unequal Predetection Signal-to-Noise Ratios," *TDA Progress Report 42-72*, pp. 95-117, Jet Propulsion Laboratory, Pasadena, California, February 15, 1983.

4. Tausworthe, R. C., "Limiters in Phase-Locked Loops: A Correction to Previous Theory," *Space Programs Summary No. 37-54*, Vol. III, pp. 201-203, Jet Propulsion Laboratory, Pasadena, California, 1968.

5. Divsalar, D., and Yuen, J. H., "Improved Carrier Tracking Performance with Coupled Phase-Locked Loops," *TDA Progress Report 42-66*, pp. 148-171, Jet Propulsion Laboratory, Pasadena, California, December 15, 1981.

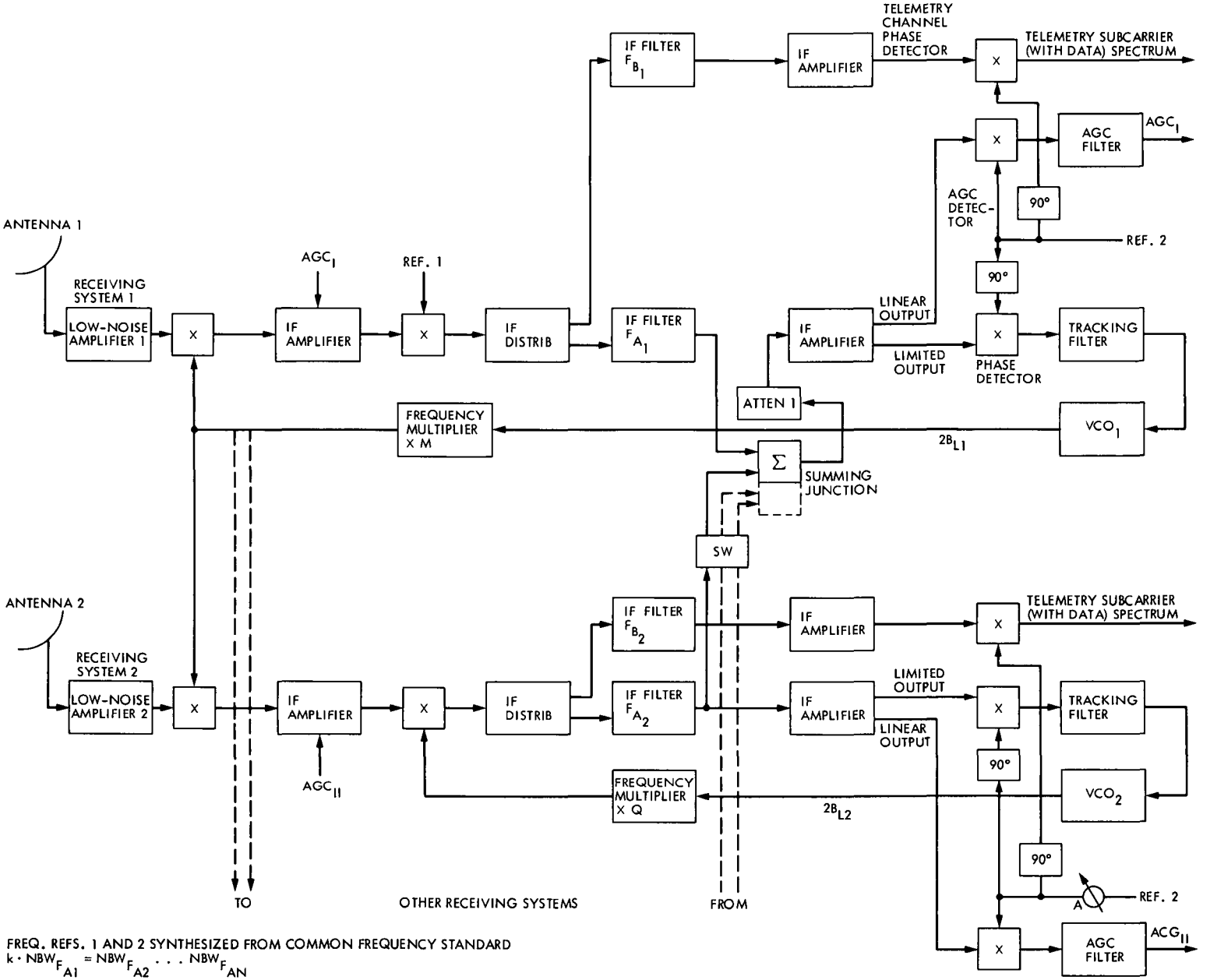

Fig. 1. Enhanced radio frequency carrier arraying

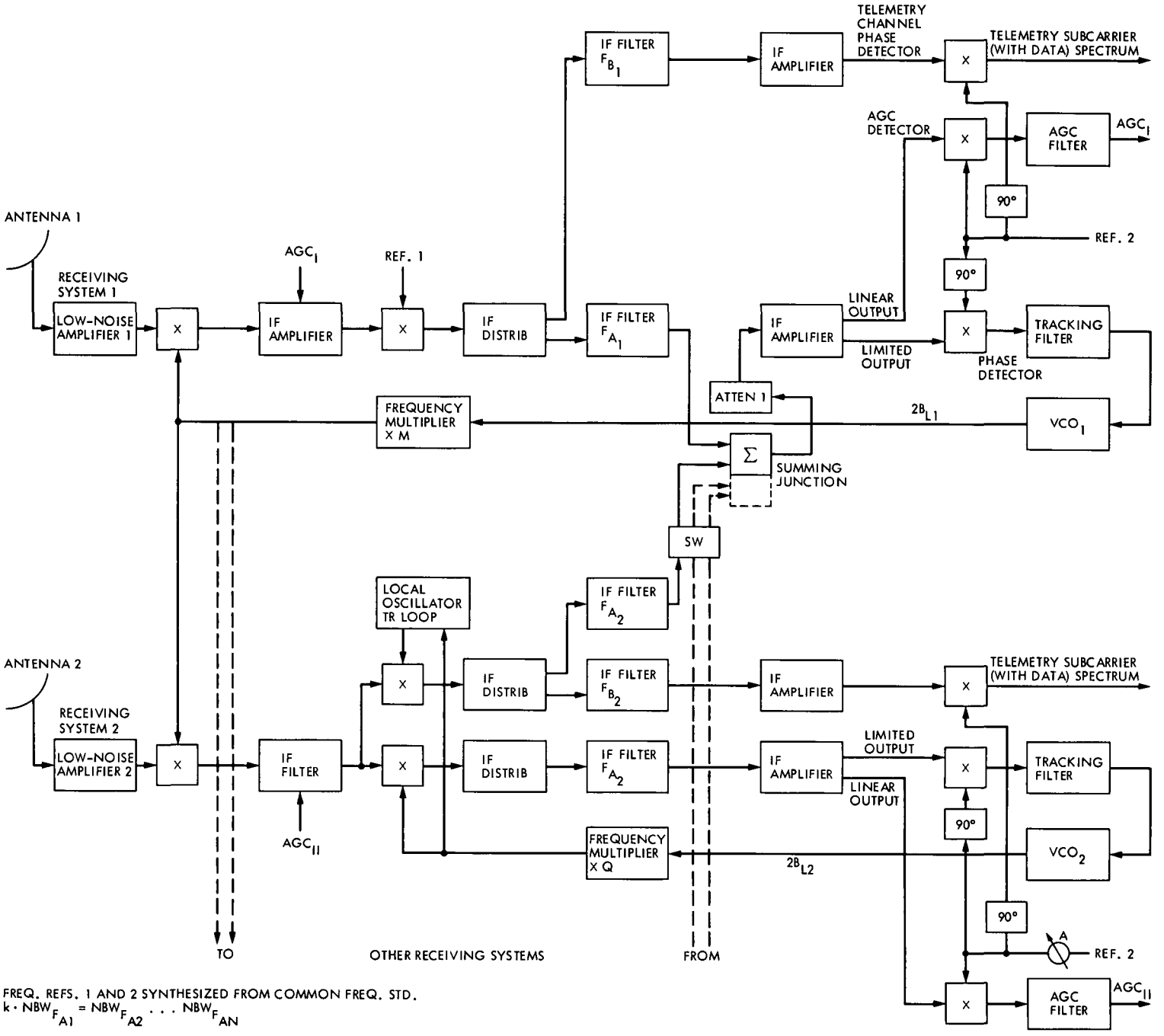

Fig. 2. Enhanced radio frequency carrier arraying with additional local oscillator filtering

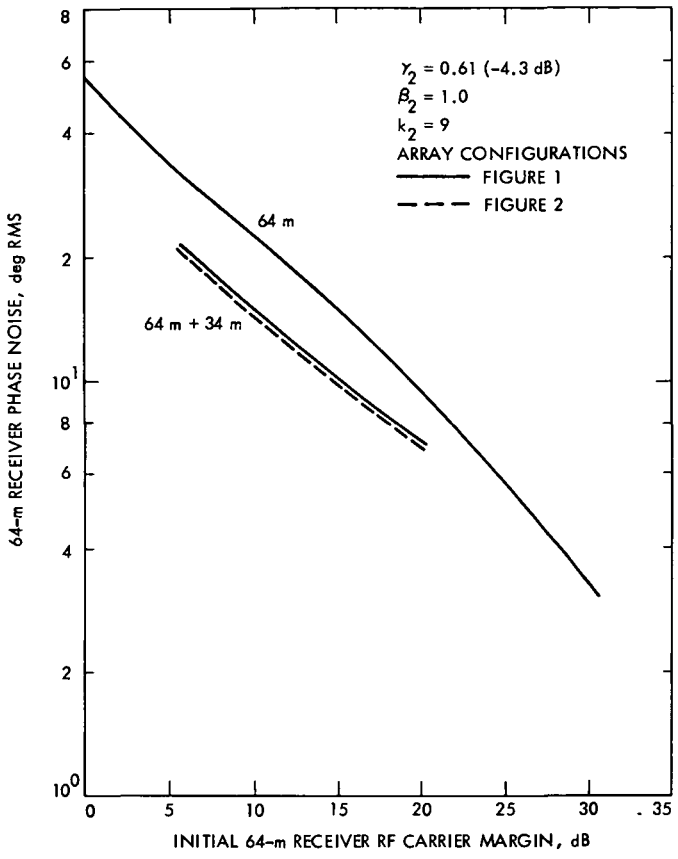

Fig. 3. 64-m receiver by itself and with enhanced RF carrier margin improvement. RF carrier tracking loop phase noise vs initial 64-m receiver carrier margin. Two receiving systems arrayed: 64-m and 34-m diameter high efficiency (listen only) ($2B_{L_{o1}}$ = 30 Hz).

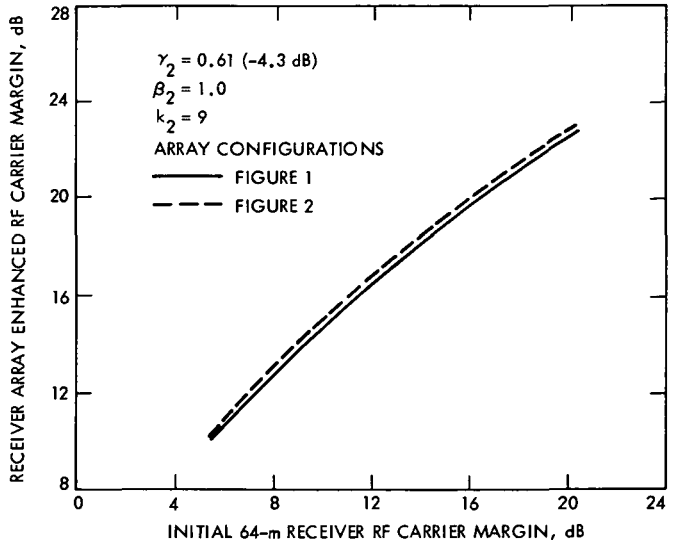

Fig. 4. Receiver array enhanced RF carrier margin vs initial 64-m receiver carrier margin. Two receiving systems arrayed: 64-m and 34-m diameter high-efficiency (listen only) ($2B_{L_{o1}}$ = 30 Hz).

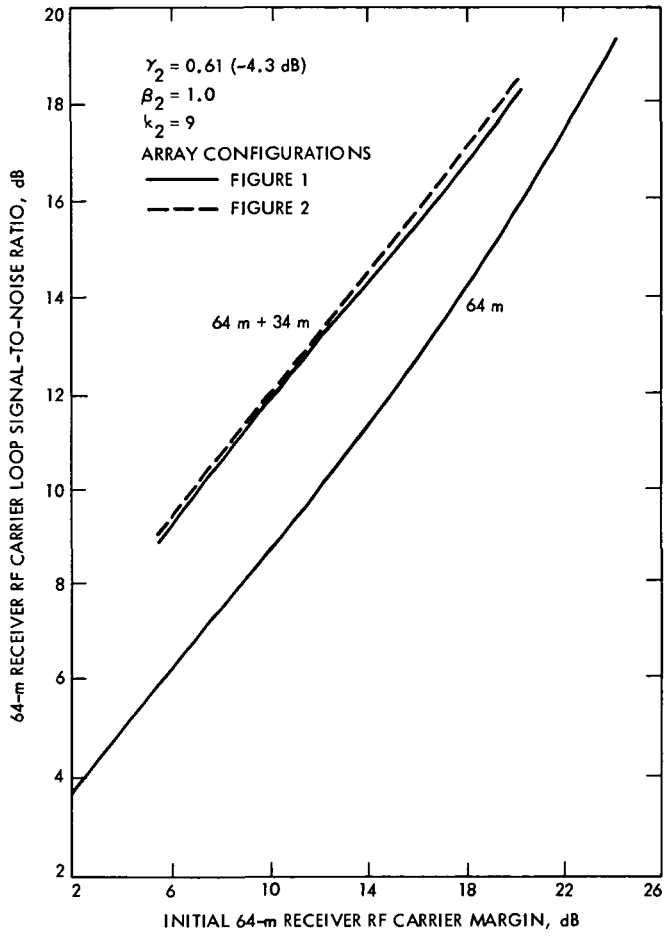

Fig. 5. 64-m receiver by itself and with enhanced RF carrier margin improvement. RF carrier tracking loop signal-to-noise ratio vs initial 64-m receiver carrier margin. Two receiving systems arrayed: 64-m and 34-m diameter high-efficiency (listen only) ($2B_{L_{o1}}$ = 30 Hz).

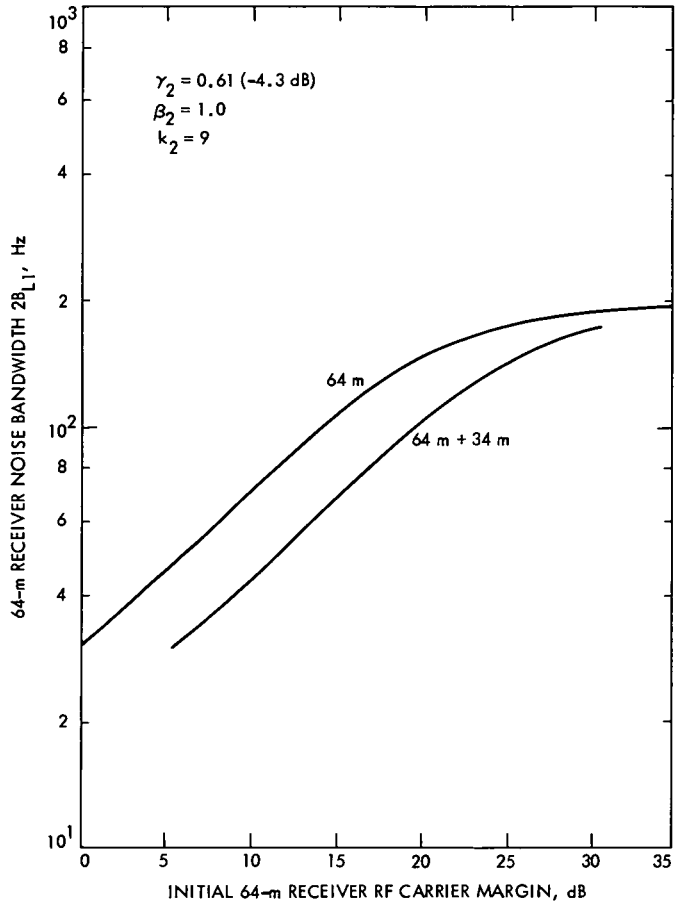

Fig. 6. 64-m receiver by itself and with enhanced RF carrier margin improvement. RF carrier tracking loop two-sided closed loop noise bandwidth vs initial 64-m receiver carrier margin. Two receiving systems arrayed: 64-m and 34-m diameter high-efficiency (listen only) ($2B_{L_{o1}}$ = 30 Hz).

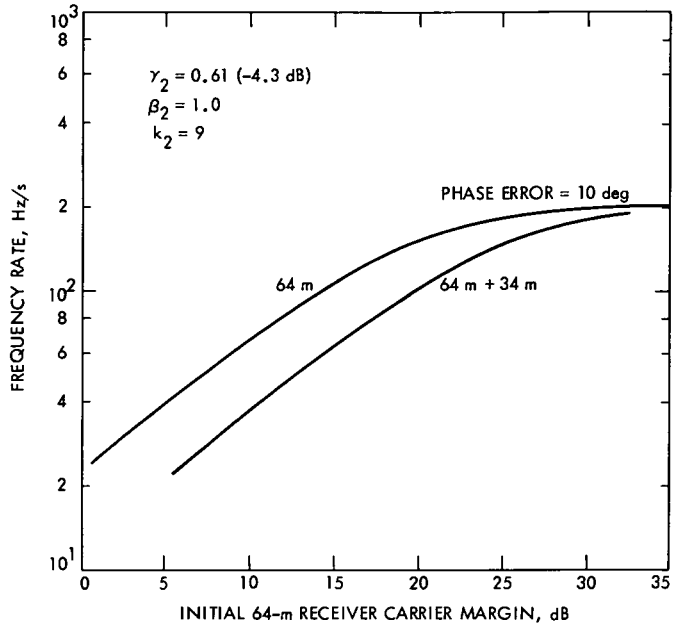

Fig. 7. 64-m receiver by itself and with enhanced RF carrier margin improvement. Frequency rate capability vs initial 64-m receiver carrier margin. Two receiving systems arrayed: 64-m and 34-m diameter high-efficiency (listen only) ($2B_{L_{o1}}$ = 30 Hz).

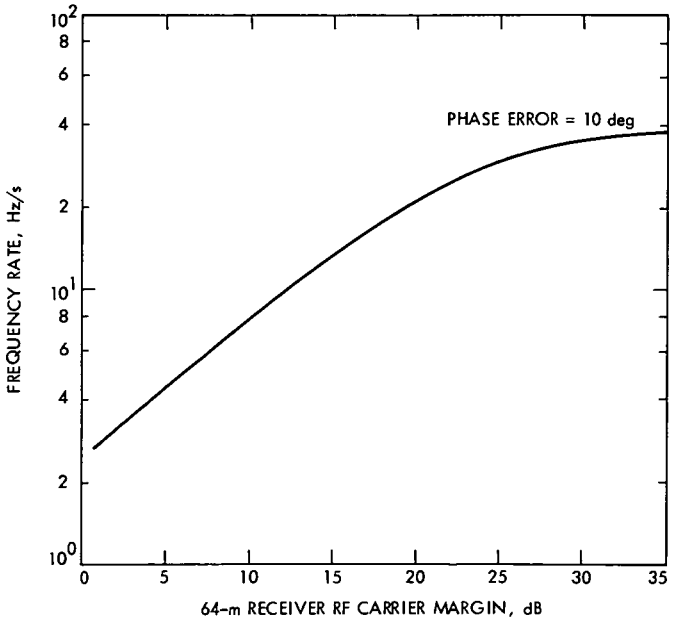

Fig. 8. 64-m receiver frequency rate capability vs RF carrier margin ($2B_{L_{o1}}$ = 10 Hz).

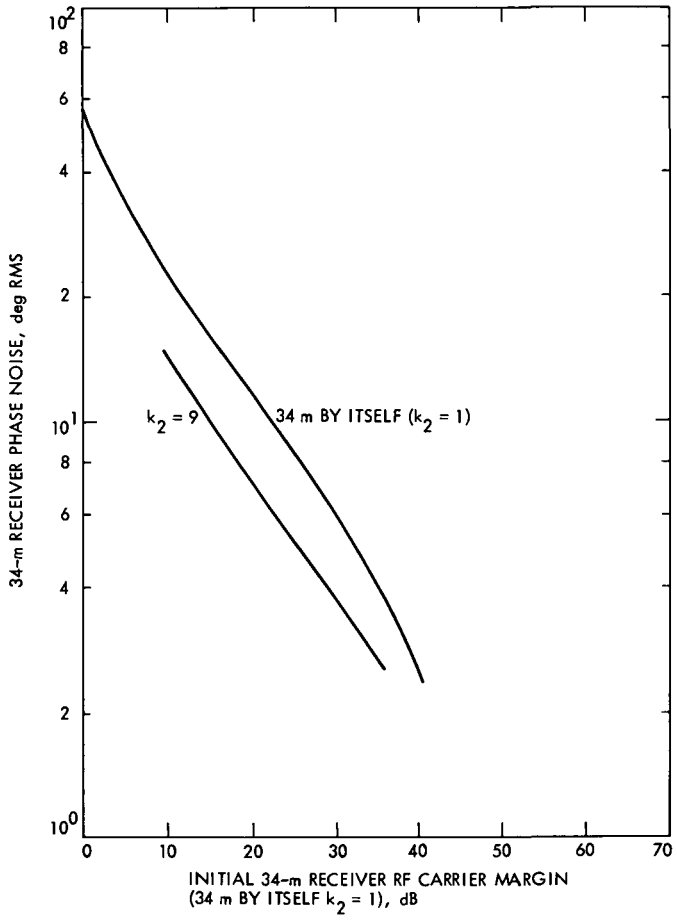

Fig. 9. 34-m receiver RF carrier tracking loop phase noise vs initial 34-m receiver carrier margin (34-m by itself $k_2 = 1$) ($2B_{L_{o2}} = 1.0$ Hz).

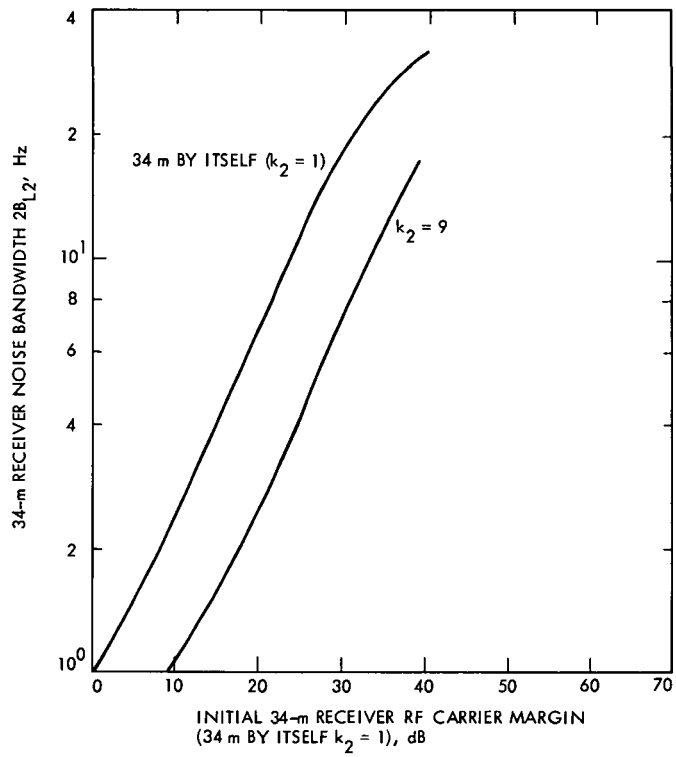

Fig. 10. 34-m receiver RF carrier tracking loop two sided closed loop noise bandwidth vs initial 34-m receiver carrier margin (34 m by itself $k_2 = 1$) ($2B_{L_{o2}} = 1.0$ Hz).